

# Bone microstructure of the sphenodont rhynchocephalian *Priosphenodon avelasi* and its paleobiological implications

SOL A. CAVASIN, IGNACIO A. CERDA, and SEBASTIÁN APESTEGUÍA



Cavasin, S.A., Cerda, I.A., and Apesteeguía, S. 2024. Bone microstructure of the sphenodont rhynchocephalian *Priosphenodon avelasi* and its paleobiological implications. *Acta Palaeontologica Polonica* 69 (1): 29–38.

Sphenodontians are a group of vertebrates with a vast taxonomic diversity and worldwide distribution of their fossils. Although they have been the subject of many studies on their phylogeny and morphology, those focused on their paleobiology are still scarce. We present here the osteohistology of eleven postcranial elements corresponding to a single specimen of *Priosphenodon avelasi*, an eilenodontine sphenodontian from Cenomanian–Turonian rocks of Río Negro (Argentina). The bone samples described here share a parallel-fibered type of matrix. The degree of vascularization varies in all the samples, but none of them present a significant density of primary vascular canals. Lines of arrested growth were observed in all appendicular elements, being better preserved in the humerus, radius and fibula. Extrinsic fibers were observed only in reduced regions of the cortex of the ulna and in one of the phalanges. The primary bone tissue suggests that the specimen had a relatively low growth rate with alternation between slow and accelerated stages. The latter could explain why this taxon reached the largest sizes of all known sphenodontians.

**Key words:** Rhynchocephalia, Sphenodontia, osteohistology, paleobiology, gigantism, Cretaceous, Argentina.

Sol A. Cavasin [sol.cavasin17@gmail.com; ORCID: <https://orcid.org/0009-0004-2890-7509>], Instituto de Investigación en Paleobiología y Geología (IIPG), Universidad Nacional de Río Negro, Av. Roca 1242, General Roca, 8332, Río Negro, Argentina; <sup>4</sup>Consejo Nacional de Investigaciones Científicas y Técnicas (CONICET)

Ignacio A. Cerda [nachocerda6@gmail.com; ORCID: <https://orcid.org/0000-0001-6279-0392>], Instituto de Investigación en Paleobiología y Geología (IIPG), Universidad Nacional de Río Negro, Av. Roca 1242, General Roca, 8332, Río Negro, Argentina; Museo Provincial Carlos Ameghino, Belgrano 1700, Paraje Pichi Ruca (predio Marabunta), 8300, Cipolletti, Río Negro, Argentina; Consejo Nacional de Investigaciones Científicas y Técnicas (CONICET).

Sebastián Apesteeguía [sebastian.apesteeguia@fundacionazara.org.ar; ORCID: <https://orcid.org/0000-0002-0414-0524>], Area de Paleontología de la Fundación de Historia Natural Félix de Azara, Universidad Maimónides, Hidalgo 775 P. 7°, C1405BCK, Ciudad Autónoma de Buenos Aires, Argentina; Consejo Nacional de Investigaciones Científicas y Técnicas (CONICET).

Received 15 March 2023, accepted 16 January 2024, published online 2 February 2024.

Copyright © 2024 S.A. Cavasin et al. This is an open-access article distributed under the terms of the Creative Commons Attribution License (for details please see <http://creativecommons.org/licenses/by/4.0/>), which permits unrestricted use, distribution, and reproduction in any medium, provided the original author and source are credited.

## Introduction

Sphenodontia is a clade of lepidosaurs currently represented by a single genus, *Sphenodon*, which is endemic to the New Zealand archipelago (Whiteside 1986; Daugherty et al. 1990). However, during the Mesozoic, this group exhibited an enormous diversity at both taxonomical and morphological levels, as well as a vast worldwide distribution (Reynoso 1996, 2003; Apesteeguía 2007, 2008; Evans and Jones 2010). The fossil record of Mesozoic sphenodontians in South America has substantially increased in recent years, with reports from rocks of the Late Triassic of Brazil and Argentina (e.g., Bonaparte and Sues 2006;

Martínez et al. 2013; Hsiou et al. 2015), Middle Jurassic of Argentina (Apesteeguía et al. 2012) and the Upper Cretaceous of Argentina (e.g., Apesteeguía and Novas 2003; Simon and Kellner 2003; Martinelli and Forasiepi 2004; Apesteeguía 2005; Apesteeguía and Rougier 2007; Apesteeguía and Jones 2012; Gentil et al. 2019). Despite the enormous taxonomic and morphological diversity of fossil sphenodontians, there are many aspects of their biology that have been poorly studied, especially those inferred from their bone microstructure (i.e., paleohistology).

Previous paleohistological contributions on sphenodontians were carried out on postcranial bones, with the sole exception of the study of LeBlanc et al. (2020) on tooth

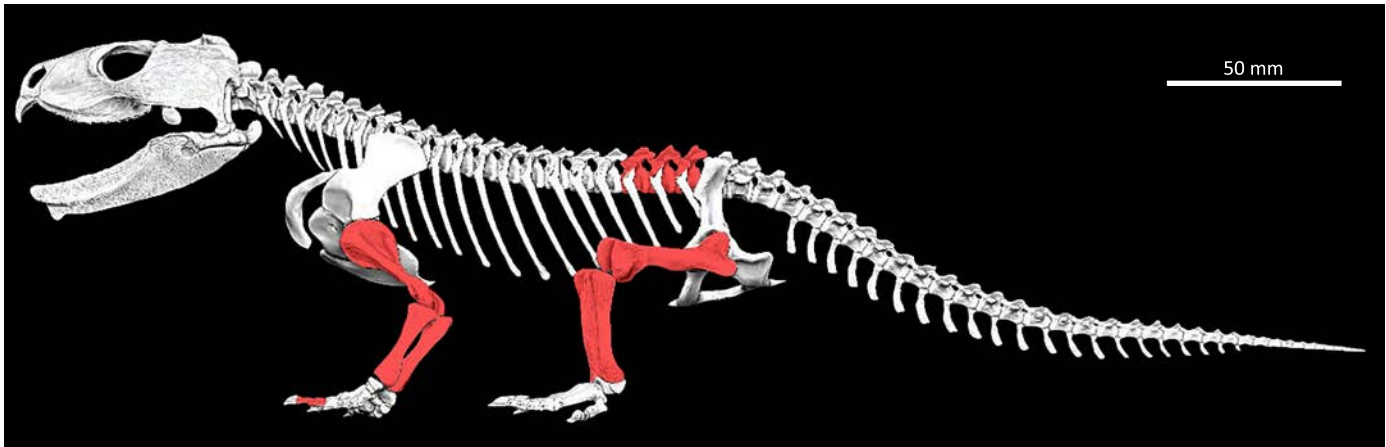


Fig. 1. Skeletal digital reconstruction of the sphenodont rhynchocephalian *Priosphenodon avelasi* Apesteguía, 2008, from northern Patagonia, late Cretaceous; by Jorge A. González showing the elements sampled for histological analysis (in red).

implantation tissues. In this regard, previous studies were done on different taxa, including *Gephyrosaurus* sp. from the Early Jurassic of England (Chinsamy and Hurum 2006), *Palaeopleurosaurus posidoniae* from the Early Jurassic of Germany (Klein and Scheyer 2017) and *Patagosphenos watuku* from the Turonian of Argentina (Gentil et al. 2019). The bone histology of *Gephyrosaurus*, which was compared with that of the first mammals, revealed the presence of parallel-fibered bone (PFB) interrupted by lines of arrested growth (LAGs). The authors also described a putative hatching line (Chinsamy and Hurum 2006). The analyzed specimens of *Palaeopleurosaurus posidoniae* showed signs of osteosclerosis in its gastralia and ribs but not in the limb bones (e.g., femur), supporting the hypothesis of aquatic specialization (Klein and Scheyer 2017). Finally, the appendicular bones of a specimen of *Patagosphenos watuku*, revealed a bone structure similar to *Sphenodon*, with the predominance of avascular PFB, presence of LAGs, presence of Sharpey's fibers, and isolated resorption cavities (Gentil et al. 2019). The authors inferred that physiological adaptations to survive in cold environments may constitute the key pre-adaptation that led to the current lineage of rhynchocephalians surviving the extinction at the end of the Cretaceous, a concept previously addressed by Apesteguía and Jones (2012) in relation to the large size of sphenodontine species.

The present work focuses on a multi-element paleohistological study carried out on a single specimen (MPCA-Pv 308) assigned to *Priosphenodon avelasi* by Apesteguía (2008), an eilenodontine sphenodontian from the Upper Cretaceous of Argentina (Apesteguía and Novas 2003). The largest known specimens of this taxon grew to one meter in length (larger than any other known sphenodontian). The main purposes of this contribution are: (i) evaluate the degree of intraskeletal histological variation; (ii) determine which of the sampled elements are most useful for skeletochronological studies (i.e., which bones preserve the best record of growth marks) and in turn compare it with other sphenodontians; (iii) evaluate the ontogenetic stage

of the *Priosphenodon* specimen MPCA-Pv 308 based on histological characteristics and how they can be correlated with morphological attributes, such as body size and the degree of neurocentral suture fusion; (iv) analyze the growth dynamics of *Priosphenodon avelasi* and (v) compare the same with other sphenodontians. The current contribution represents the first multi-element paleohistological study carried out on an extinct sphenodontian.

*Institutional abbreviations.*—MPCA-Pv, Museo Provincial Carlos Ameghino, Cipolletti, Río Negro Province, Argentina.

*Other abbreviations.*—CGM, cyclical growth marks; ICL, inner circumferential layer; LAGs, lines of arrested growth; PFB, parallel-fibered bone.

## Material and methods

A total of eleven thin sections from different elements of the postcranial skeleton of a single specimen of *Priosphenodon avelasi* (MPCA-Pv 308) were analyzed (Fig. 1). The specimen was previously assigned to *Priosphenodon avelasi* by Apesteguía (2008). All appendicular sections were made at the mid-diaphysis level, including left and right humerus, radius, ulna, left and right femur, tibia, fibula, two undetermined phalanges from the forelimb, as well as half of a neural arch and vertebral centrum of a presacral vertebra (Fig. 2).

The specimen studied here presents a dentary with a length of approximately 60 mm, which would correspond to a young adult ontogenetic stage, as proposed by Apesteguía (2008). This size represents 40% of the largest known individual size. Likewise, in the preserved vertebrae, well-marked sutures can be observed as a consequence of an incomplete fusion of the neural arches to the vertebral centra. Compared to other species, the individual, which includes a complete skull, was found at the fossiliferous locality of La Buitrera (Río Negro Province), in outcrops of the Candeleros Formation (Cenomanian–Turonian; Leanza et al. 2004).

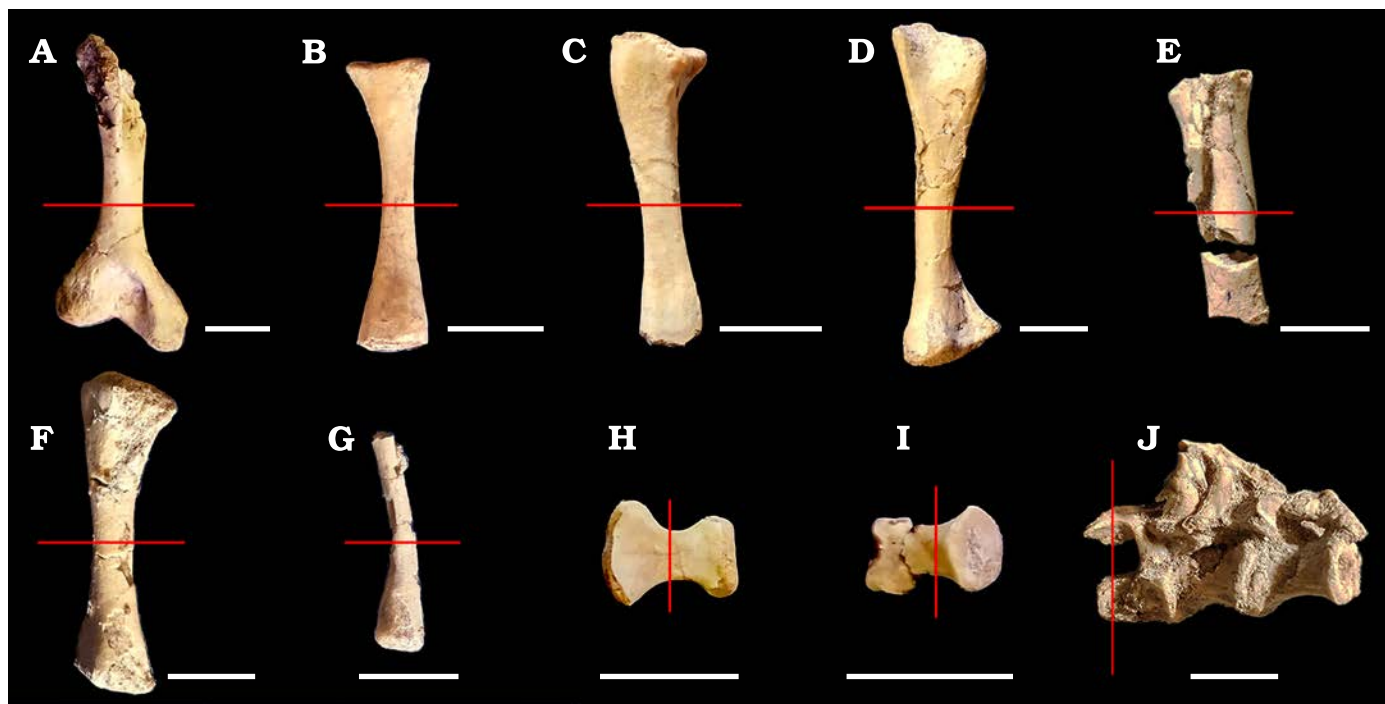


Fig. 2. Appendicular and axial bones of the sphenodont rhynchocephalian *Priosphenodon avelasi* Apesteguía, 2008 (MPCA-Pv 308) from northern Patagonia, late Cretaceous, sampled for histological analysis. **A.** Right humerus in anterior view (an image of the left humerus was not processed due to its fragmentary state). **B.** Left radius in anterior view. **C.** Left ulna in anterior view. **D.** Left femur in lateral view. **E.** Fragmented right femur. **F.** Tibia in anterior view. **G.** Fragment of fibula in anterior view. **H, I.** Phalanges in dorsal view. **J.** Articulated presacral vertebrae in right lateral view. Scale bars 10 mm.

All samples were processed in the Paleohistological Laboratory of the Museo Provincial Carlos Ameghino (Cipolletti, Río Negro Province, Argentina) and were prepared following the methodology proposed by Cerda et al. (2020). For the majority of the elements (surfaces with a diameter between 10 and 20 millimeters), a small sample was obtained for making thin cuts while leaving the majority of the original piece intact. Before making the cut, the bone surface was cleaned with alcohol and then covered with a two-part epoxy putty layer. Once the protective layer reached the desired hardness, a cut could be made using a diamond cutting saw, leaving a small portion uncut to be broken. Once the bone sample was removed, a silicone rubber mold and a replica made of water-based acrylic resin were created to prevent the loss of anatomical information for future studies and to ensure minimal intervention with the bone remains.

The next step was to place the sample in a container made of thick aluminum foil and embed it in DICAST LY 554 epoxy resin with DICURE Hy 554 catalyst in a ratio of 100:20, and then let it cure on a hot plate for 24 hours. The resulting block was cut with a diamond saw to obtain two or more flat surfaces, each of which exhibited a certain degree of porosity. Since filling these spaces is strictly necessary for the proper mounting of the sample, each surface was coated with DICAST LY 867 epoxy resin combined with DICURE hY 867 catalyst in a ratio of 100:60, using a spatula. Once the resin had completely permeated the surface, a final polish was performed with abrasive powders (silicon carbide) of different granulometries on a homemade lapi-

dary grinding machine or a glass plate until the surface was completely smooth and material could be observed under the light of an optical microscope.

A detailed description of the tissues was made with a binocular optical and petrographic polarized light microscope, based on: the presence and distribution of primary and secondary tissues, the degree of arrangement of intrinsic collagen fibers, type of vascular canals (primary or secondary), degree of vascularization, orientation of vascular canals, presence and distribution of extrinsic fibers (i.e., Sharpey's fibers) and number and distribution of cyclical growth marks (CGM), including annuli and lines of arrested growth (LAGs). For LAG identification, we considered clear interruptions of the primary bone tissue that were present around the entire preserved cortex. For LAG counting, direct observations of the sections were combined with high definition composite images. Nomenclature and definitions of structures used in this study are derived from Francillon-Vieillot et al. (1990) and Buffrénil and Quilhac (2021). In the case of the term "intrinsic fibers", we follow the definition of Ricqlès et al. (1991), for which this term refers to the collagenous fibers that are deposited by osteoblasts. To evaluate variation in bone compactness, we conducted a quantitative analysis of the elements. For this, images obtained from the sections were digitally transformed into black and white (black for bone and white for internal spaces) using Photoshop CS4. Once the images were processed, Image J (Rasband 2003) was used to calculate the compaction index (expressed as the percentage occupied by bone tissue in a given area).

## Results

*Humerus.*—Both humeri present a relatively thick and compact cortex (Fig. 3A<sub>1</sub> and A<sub>2</sub>). The medullary territory exhibits several resorption cavities of different shapes and sizes. The compact bone is mainly formed by primary bone tissue. The matrix mostly exhibits mass birefringence and contains abundant osteocyte lacunae with fusiform aspects and a good degree of spatial organization (Fig. 3A<sub>3</sub>). These features correspond to a matrix of parallel-fibered bone. Vascularization is relatively scarce, represented by radial and, to a lesser degree, longitudinal canals (Fig. 3A<sub>4</sub>). Resorption cavities are small and they are mostly formed in the perimedullary region of cortex. One of the sections exhibits a prominent invagination in one of the lateral regions of the outer cortex, which is attributed to the presence of a nutrient canal (Fig. 3A<sub>1</sub>). In both sections, well defined LAGs were distinguished, observing a total of thirteen in both humeri. The seven LAGs observed in the outer half can be followed throughout the entire sample without presenting interruptions. The remaining six are closer to the medullary region, so they are interrupted by resorption cavities (Fig. 3A<sub>4</sub> and B<sub>1</sub>). The spacing between successive LAGs is not homogenous in the first eight LAGs (i.e., counting from the inner cortex). Additional possible growth lines that form complexes of double or triple LAGs were observed in some areas. Nevertheless, since the same are only present in portions of the cortex, we don't consider them to be true LAGs. Both samples reveal the presence of thick layers in which the tissue exhibits a higher spatial organization of the osteocyte lacunae and a lower density of the vascular canals, which are even absent in some areas (Fig. 3A<sub>5</sub>). A total of five of these layers of poorly vascularized bone tissue, which does not correspond with true annuli, are recorded in both elements. Of these five layers, the one that exhibits the greatest thickness is located in the outermost cortex.

*Radius.*—The thin section (Fig. 3B<sub>1</sub>) of this bone consists of an avascular cortex formed by parallel-fibered bone, which contains abundant lacunae of spindle-shaped osteocytes concentrically arranged (Fig. 3B<sub>2</sub>, B<sub>3</sub>). Branched canaliculi that interconnect these lacunae are well preserved in certain regions. The sample presents a free medullary cavity (that is, without spongy tissue) and the perimedullary region is partially lined by a layer of secondary lamellar bone tissue (inner circumferential layer, ICL). This layer has been partially eroded during the expansion of the medullary cavity, which appears to be asymmetrical. A total of twelve well-defined LAGs are preserved. Whereas the outer six LAGs can be traced around the entire cross section, the others have been partially eroded as a consequence of the resorption of the medullary cavity (Fig. 3B<sub>1</sub>). A noticeable variation is observed in the spacing between the first seven LAGs.

*Ulna.*—This sample presents a free, well-developed medullary cavity encircled by a thick cortex of compact bone (Fig. 3C<sub>1</sub>). The compacta are mostly formed by poorly vas-

cularized parallel-fibered bone. Although the osteocyte lacunae are mostly spindle-shaped and show an ordered spatial arrangement, they have a more globular appearance and a chaotic arrangement in the lateral region of the bone element. These particular areas of the cortex are also characterized by the abundance of Sharpey's fibers (Fig. 3C<sub>2</sub>), which cross the bone surface obliquely. The cortical bone is interrupted by at least twelve LAGs. A noticeable separation is observed between the fifth and sixth LAG. Seven LAGs are roughly grouped in the outer third of the compacta. From these, the spacing is rather homogenous among the last five. The five LAGs located toward the perimedullary region have been partially eroded by the asymmetrical expansion of the medullary cavity (Fig. 3C<sub>3</sub>). Few resorption cavities are scattered around the medullary cavity. These cavities exhibit variable sizes and are internally lined with secondarily formed lamellar tissue.

*Femur.*—Both femora exhibit a prominent medullary cavity surrounded by a poorly vascularized cortex formed by parallel-fibered bone. The degree of vascularization is low in both samples, with scattered longitudinal canals being observed. Noticeably large resorption cavities are observed in the perimedullary region. These are usually lined with secondary lamellar tissue. Twelve LAGs are well-defined in one of the samples and in the other, which has a poor preservation, only five are well-defined (see SOM: fig. S1A, B, Supplementary Online Material available at [http://app.pan.pl/SOM/app69-Cavasin\\_etal\\_SOM.pdf](http://app.pan.pl/SOM/app69-Cavasin_etal_SOM.pdf)). The most important variation regarding the spacing between growth marks is observed in the first six LAGs, particularly between the second and third, and between the sixth and seventh. The first two LAGs are almost entirely eroded due to the expansion of the medullary cavity. Variation in the degree of vascular density and osteocyte lacunar density as described for the humeri is observed in the compacta, but their distribution is much more diffuse.

*Tibia.*—The cortex exhibits a considerable degree of vascularization, which consists of abundant canals oriented both radially and longitudinally. These canals exhibit a rather heterogenous spatial distribution. The cortex is formed by parallel-fibered bone, which contains abundant osteocyte lacunae. Except for the most vascularized regions, the osteocyte lacunae exhibit a rather organized pattern of arrangement. The perimedullary region contains numerous resorption cavities of variable sizes and shapes. These cavities are lined by lamellar bone tissue. A total of twelve LAGs were observed, of which seven are found between the periosteal and middle regions of the cortex and can be followed throughout the entire cross section (see SOM: fig. S1C, D). The remaining five are found closer to the medullary region for which they are mostly interrupted, as seen in previous samples. The distance between successive LAGs is variable in the sample.

*Fibula.*—The sample has an avascular and relatively thick cortex, with a free medullary cavity (Fig. 3D). The peri-

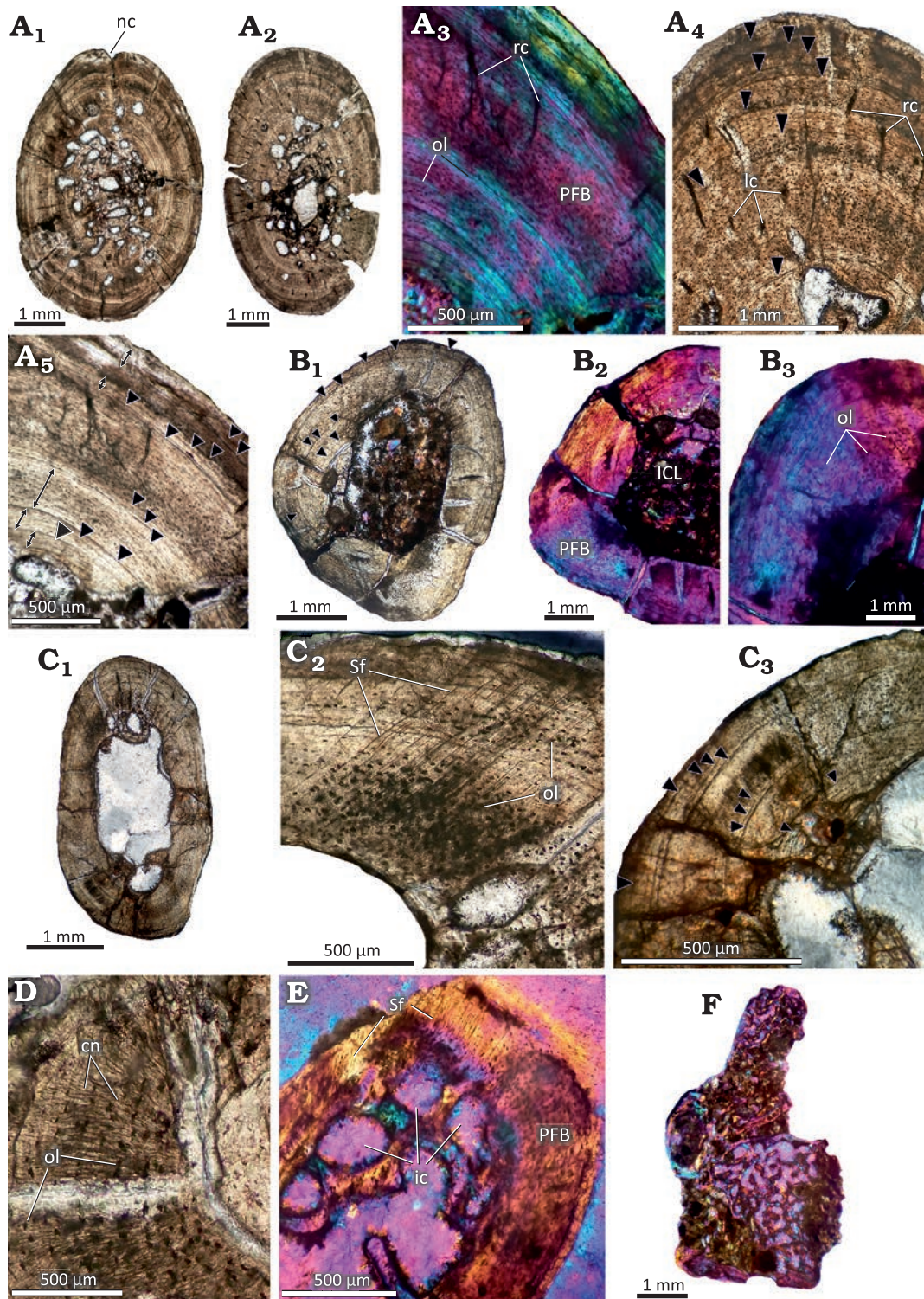


Fig. 3. Postcranial histology of the sphenodont rhynchocephalian *Priosphenodon avelasi* Apesteguía, 2008 (MPCA-Pv 308) from the Upper Cretaceous Candeleros Formation, Argentina. Black arrowheads signal the position of LAGs. **A.** Bone histology of the humeri. A<sub>1</sub>, A<sub>2</sub>, complete cross sections; A<sub>3</sub>–A<sub>5</sub>, detailed views of the cortex showing predominance of poorly vascularized parallel fibered bone and distribution of LAGs; A<sub>4</sub>, detail of the cortex showing primary vascular canals and LAGs; A<sub>5</sub>, regions of the cortex marked with double arrows where the tissue presents a better organization and LAGs. **B.** Bone histology of the radius. B<sub>1</sub>, general view; B<sub>2</sub>, B<sub>3</sub>, details. Note the absence of vascular canals and the mass birefringence of the primary bone tissue. **C.** General view of the ulna. C<sub>1</sub>, general view; C<sub>2</sub>, C<sub>3</sub>, detailed views showing abundant Sharpey's fibers (C<sub>2</sub>) and distribution of LAGs (C<sub>3</sub>). **D.** Detailed view of the cortex of the fibula showing canaliculi and osteocyte lacunae. **E.** Detailed view of the cortical bone in the phalange "A" showing abundant Sharpey's fibers. **F.** General view of the presacral vertebra section. Note the predominance cancellous bone tissue. A<sub>1</sub>, A<sub>2</sub>, A<sub>4</sub>, A<sub>5</sub>, B<sub>1</sub>, B<sub>3</sub>, C, D, normal transmitted light; A<sub>3</sub>, B<sub>2</sub>, E, F, cross polarized light with lambda filter. Abbreviations: cn, canaliculi; ic, intertrabecular cavities; ICL, inner circumferential layer; lc, longitudinal canals; nc, nutrient canal; ol, osteocyte lacunae; PFB, parallel fibered bone; rc, radial canals; Sf, Sharpey's fibers.

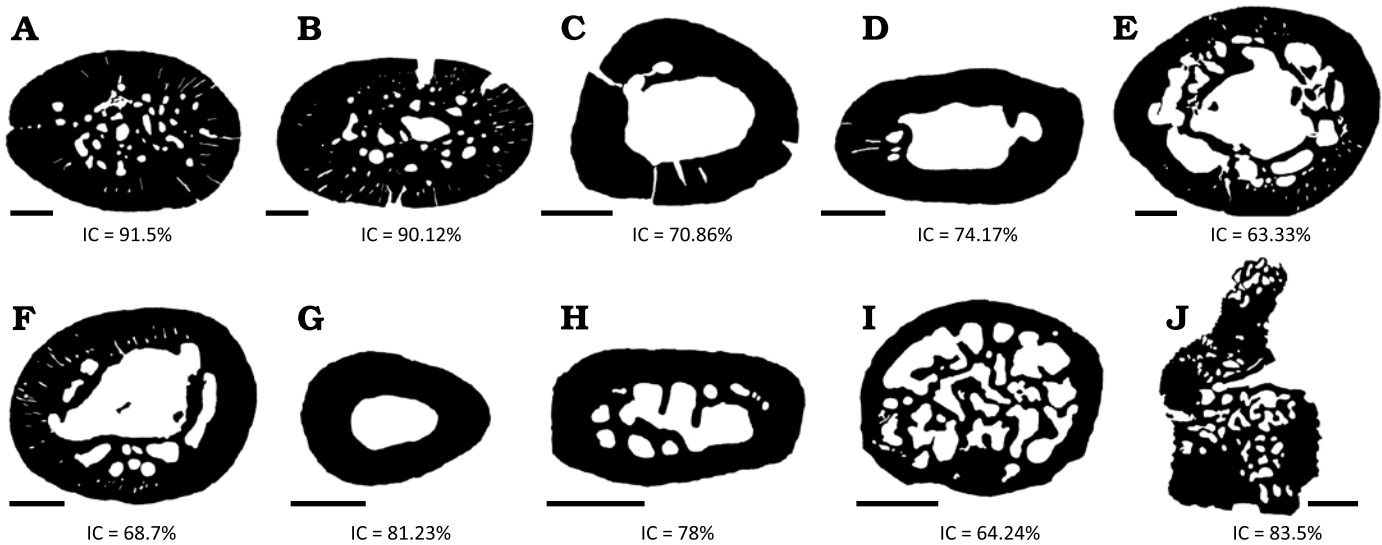


Fig. 4. Compaction index (CI) of several of the histological sections analyzed here from *Priosphenodon avelasi* (northern Patagonia, late Cretaceous). Note the high degree of compaction that both humeri present in comparison with the rest of the bone elements. A. Right humerus. B. Left humerus. C. Left radius. D. Left ulna. E. Right femur. F. Tibia. G. Fibula. H, I. Phalanges. J. Articulated presacral vertebrae. Scale bars 1 mm.

medullary margin preserves the remains of ICL composed of secondary lamellar tissue, which is not fully preserved due to the asymmetric displacement of the medullary cavity. The cortex is formed by parallel-fibered bone, which is mostly birefringent, with concentrically oriented fusiform osteocyte lacunae. Canaliculi are well preserved in several regions (Fig. 3D). A total of thirteen LAGs are preserved. From these, only the last seven LAGs can be traced around the whole cortex. The remaining growth marks are partially eroded by the asymmetrical expansion of the medullary cavity. Whereas the spacing between the last seven LAGs is roughly homogeneous, this distance is strongly variable between the other growth marks.

**Phalanges.**—Sections from two phalanges (here designated as A and B for descriptive purposes) were analyzed. Both samples are formed by avascular parallel-fibered bone. This pattern is interrupted in one of the regions of the sample A by the presence of Sharpey's fibers, which are obliquely oriented with regard to the outer surface (Fig. 3E). The sample A has a relatively thick cortex, which encircles a medullary region partially filled with cancellous bone. The resorption cavities are large and they are lined by secondary lamellar tissue. Remains of primary bone tissue are also observed. The cortical bone is interrupted by at least ten poorly preserved LAGs (see SOM: fig. S1E). Sample B, unlike sample A, has a relatively thin cortex with a prominent medullary cavity, which is filled with secondary spongy bone. The bony trabeculae are formed by secondary lamellar bone and they delimitate large intertrabecular spaces. A total of eight LAGs were recorded in this sample, most of which are faintly preserved. No LAG could be traced along the entire section (see SOM: fig. S1F).

**Presacral vertebra.**—The sample corresponds to half of a centrum and neural arch (Fig. 3F). The element is composed

of spongy tissue, which has numerous intertrabecular spaces formed by lamellar bone of secondary origin. Cortical tissue is preserved only in reduced areas and appears to be formed by parallel-fibered bone. The poor preservation of the material did not allow for a better characterization.

**Compaction index (CI).**—For all the elements described from the appendicular skeleton, the CI was higher than 50%, presenting a well-developed and poorly vascularized cortex. It should be noted that both humeri presented the highest CI (higher than 90%) (Fig. 4).

## Discussion

**Intraskelletal variation.**—Although the sampled elements exhibit a roughly homogeneous bone microstructure, there are variations with respect to particular histological characteristics, including degree of vascularization, compactness, presence of Sharpey's fibers and number of CGMs. With exception of the tibia, which contains a moderate number of vascular canals, the degree of vascularization is clearly higher in stylopodial than zeugopodial and autopodial bones, which include avascular elements as fibula and phalanges. This variation is possibly related to the relative size of the elements. With the exception of the tibia, the zeugopodial and autopodial bones are also characterized by the small diameter of their diaphyses in comparison with autopodial elements. Following Ricqlès and Gayon (2015), this variation may be explained by the specific growth dynamics of different bones within an individual skeleton. In this regard, if a small autopodial bone takes the same amount of time to reach its adult size than the much larger stylopodial element in the same individual (growth isochrony), it makes sense that different tissue types originated from different growth rates will be laid down in the different bones (Ricqlès and

Gayon 2015). Since the degree of vascularization is positively correlated with the rate of bone apposition (Castanet et al. 2000), poorly vascularized tissues would prevail in the smaller bones, and well vascularized ones in the larger.

The CI in all the elements is higher than 60%, and the humerus is the one that shows the higher percentages (>90%). This notable difference with the other samples could be related to a greater biomechanical load that the animal exerted on the humeri as a result of, for example, a high level of burrowing activity. ‘Wolff’s Law’ postulates that bone increases in density and cortical thickness in response to the loads to which an individual is subjected throughout its life (Meier et al. 2013).

However, although this is not enough to establish a direct relationship between compaction and a possible burrowing habit in this taxon, both its anatomical features as well as environmental and sedimentological evidence strongly support burrowing activities (Apesteguía 2008). Added to this are the burrows of fossil tetrapods in Cretaceous rocks in the province of Chubut (Argentina) described by Melchor et al. (2023). Fossil burrow casts preserved in a paleosol are composed of a ramp with no enlargement, showing a reniform cross-section. The shape of the burrow casts (i.e., strongly horizontally widened in cross section) and comparisons with modern lizard burrows suggest that the producers were lepidosaurs, probably eilenodontine sphenodontians. It is worth mentioning that the CI of the *Priosphenodon avelasi* humerus is larger than those reported for other sphenodontian taxa, including *Sphenodon punctatus* (CI ~80) and *Palaeopleurosaurus posidoniae* (CI = 85) (Klein and Scheyer 2017).

Other intraskeletal histological variation has been found with regard to the distribution of Sharpey’s fibers. These extrinsic fibers were only found in very small sectors of the cortex of the ulna and one of the phalanges. Since Sharpey’s fibers are associated with insertion regions of soft tissues such as muscles, tendons and ligaments (Francillon-Vieillot et al. 1990), their particular distribution in *Priosphenodon avelasi* MPCA-Pv 308 is possibly due to the presence of specific muscles in this taxon. For example, the Sharpey’s fibers recorded in the phalanges possibly correspond to the retractor tendons of the toes (Castanet et al. 1988). As occurs in other taxa (e.g., Pereyra et al. 2019), the identification of these fibers in different parts of the skeleton of *Priosphenodon avelasi* could help establish muscle insertion sites in future studies.

The last parameter that exhibits clear intraskeletal variation corresponds to the number of preserved LAGs. These cyclical growth marks were identified in all histological sections except the neural arch and centrum of the vertebra, due to the poor conservation of primary bone. The observed number of these growth marks varies between eight and thirteen, with the highest number observed in both humeri and the fibula. This variation is possibly related to the degree of expansion of the medullary cavity, which has been previously reported in reptiles by Griffiths (1961) and

Hutton (1986). In the case of *Priosphenodon avelasi*, the degree of medullary expansion was low in the humerus and fibula. An alternative hypothesis for the intraskeletal histological variation of LAGs in the sampled elements is the one proposed by Castanet et al. (1988), who suggest that the growth of some skeletal elements lasts longer than others (bone heterochrony). In the case of *Priosphenodon avelasi*, this variability in the growth rate is clearly reflected in the humerus and fibula, which present a wider primary cortex, which allowed a greater number of LAGs (thirteen) to be conserved compared to with other elements such as the phalanges, which had a smaller number (eight and ten).

Variation in LAG counts between different elements of the same individual has been documented in several instances (e.g., Horner et al. 1999; Waskow and Sander 2014; Ponce et al. 2022), including in *Sphenodon* (e.g., Castanet et al. 1988; Schucht et al. 2021). Since cyclical growth marks (i.e., LAGs and annuli) correspond with annually formed structures (e.g., Castanet et al. 1993), the determination of which element preserves the highest number is important to age estimations. In the case of *Priosphenodon avelasi*, the humerus and fibula appear to be the best elements for age estimations, which was thirteen in both elements for MPCA-Pv 308. Since both humeri and fibula exhibit a free medullary cavity, which implies that early formed LAGs have been eroded, the age estimated is necessarily a minimum age.

**Sexual and somatic maturity.**—Considering that sexual maturity occurs well before the end of the growth in living reptiles, including *Sphenodon* (Castanet et al. 1988), the same can be assumed with a high degree of certainty for *Priosphenodon*. Since sexual maturation can affect appositional bone growth in vertebrates, the first can be inferred from osteohistological data (e.g., Chinsamy-Turan 2005; Huttenlocker et al. 2013; Erickson 2014). The spacing pattern of LAGs is of special importance to assess growth dynamics. Generally, in the early stages of development the growth marks are widely spaced, and the spacing decreases suddenly to then remain relatively close and constant for long periods of time (Buffrénil and Quilhac 2021). This pattern is found in taxa with indefinite growth (numerous amphibians and reptiles), in which there is a sharp drop in growth rate after reaching sexual maturity (Caetano 1990; Montori 1990) accompanied by a change in the organization of intrinsic fibers (from disorganized to well organized, from vascularized to poorly vascularized) (e.g., Castanet and Baez 1991; Khonsue et al. 2010). Considering the elements with the best growth records in MPCA-Pv 308, the last four LAGs are closely spaced. Also, these growth marks are formed in region in which intrinsic fibers exhibits a relatively high degree of spatial organization, as can be seen primarily in the humeri. In this region, the tissue presents osteocyte lacunae with better spatial organization and the absence of vascular canals. These features suggest that the individual MPCA-Pv 308 reached or was close to reaching sexual maturity before death.

Regarding somatic maturation, the same is more difficult to establish in our sampled individual. Although somatic maturity can be assessed for several tetrapod groups from the presence of an external fundamental system (i.e., poorly vascularized or avascular layer of bone composed of slowly deposited parallel-fibered or lamellar tissue) in the subperiosteal cortex (Horner et al. 1999; Chinsamy-Turan 2005), such structure has not been recorded in lepidosaurs to date (Buffr enil and Houssaye 2021). In *Sphenodon*, the assumed growth by bone apposition resulted from somatic maturation does not seem to leave any particular histological structure (Castanet et al. 1988). Taking into account the size of MPCA-Pv 308, it appears that the same corresponds to a still growing individual, which agrees with the young adult stage inferred a priori from gross morphology. Likewise, the presacral vertebrae of the specimen do not show a complete fusion of the neural arches to the vertebral centra, leaving well marked sutures that can be distinguished with the naked eye. Although this last parameter is not well established for the clade, it may be that in *Priosphenodon* sexual maturity is reached long before the complete fusion of the neurocentral sutures. Comparing with *Sphenodon*, in which sexual maturation is attained when the individuals reach approximately 75% of the adult size, *Priosphenodon* exhibits a considerably early onset of sexual maturation.

**Growth dynamics.**—The bone matrix that predominates in all the analyzed histological sections corresponds to parallel-fibered tissue with a mineralization rate of 0.1 and 0.5  $\mu\text{m}/\text{day}$  (Chinsamy-Turan 2005). It is considered as an intermediate between the lamellar matrix (linked to slow growth of bone tissue) and the woven-fibered matrix (linked to fast growth). In this sense, *Priosphenodon avelasi* does not differ notably from other fossil sphenodontians, such as *Palaeopleurosaurus posidoniae* (Klein and Scheyer 2017), *Gephyrosaurus* sp. (Chinsamy and Hurum 2006), and *Patagosphenos watuku* (Gentil et al. 2019), or as *Sphenodon punctatus* (Castanet et al. 1988). An important difference occurs, however, with regard to the degree of vascularization among sphenodontians. While the stylopodial bones of *Priosphenodon avelasi* and *Palaeopleurosaurus posidoniae* exhibit some degree of vascularization, these bones are avascular in *Sphenodon punctatus* and *Gephyrosaurus* sp. (the histology of *Patagosphenos* is known from a single fibula and a metatarsus, which difficult its comparison with other taxa than *Priosphenodon*). Taking into account the relative distance between growth marks, *Priosphenodon avelasi* has irregularly spaced LAGs like other fossil forms (i.e., *Gephyrosaurus* sp., *Patagosphenos watuku*, and *Palaeopleurosaurus posidoniae*). This was interpreted as an indicator that the growth rate experienced important variations throughout ontogeny (Klein and Scheyer 2017). The opposite occurs in *Sphenodon*, which presents a regular spacing between LAGs and is associated with little variation in growth rates (Castanet et al. 1988).

The growth dynamic of *Priosphenodon* inferred from its long bone microstructure provides valuable data with regard to the body size of the taxon, which represents a case of gigantism within Sphenodontia. Compared with *Sphenodon*, which is characterized by an avascular cortical bone with closely spaced LAGs, *Priosphenodon* exhibits moderate vascularization in stylopodial and some zeugopodial bones and a noticeable increase in LAG spacing in certain areas of the cortex. These features suggest that the large body size of *Priosphenodon* was not achieved by a prolonged slow growth. Instead, the growth was faster than in other small bodied forms. In addition, the distinct increase in the distance between LAGs in some areas of the cortex indicates that *Priosphenodon* had the capability to undergo periods of relatively faster growth. These variations in the spacing of growth marks have been explained in some cases as responses to environmental fluctuations (Buffr enil and Castanet 2000).

## Conclusions

Here we conducted the first multi-element paleohistological study carried out on an extinct rhynchocephalian. Long bone histology reveals that *Priosphenodon avelasi* MPCA-Pv 308 attained a minimum age of thirteen years. This individual appears to be a subadult specimen, since histological features indicate that it reached sexual but not somatic maturation, which concurs with the presence of neurocentral sutures that are not fully fused. The humerus and radius have a better preservation of growth marks and, hence, are better for skeletochronological studies. The predominance of parallel-fibered bone tissue indicates that *Priosphenodon avelasi* exhibited a relatively low growth rate, which is a conservative trait within Sphenodontia. Such a growth rate, however, was not constant over time. In this regard, the growth of *Priosphenodon avelasi* alternates between slow and fast periods. These periods of rapid growth in *Priosphenodon avelasi* could have led to the gigantism attained by this species, which has not been reported, up to now, in any other rhynchocephalian.

## Acknowledgements

We thank the authorities of the Instituto de Investigaci n de Paleobiolog a y Geolog a (IIPG) (General Roca, R o Negro, Argentina) and the Carlos Ameghino Provincial Museum (Cipolletti, R o Negro, Argentina) for having provided the necessary facilities and instruments to carry out this work. We thank Jorge Gonz lez, for the scientific illustration of the complete skeleton of *Priosphenodon avelasi*. Finally, we appreciate the comments and observations of the reviewers Christian Heck (Pacific Northwest University of Health Sciences, Yakima, USA) and Jordi Alexis Garcia Mars  (Museo Argentino de Ciencias Naturales “Bernardino Rivadavia”, Buenos Aires, Argentina), which helped improve the manuscript. The following projects provided financial support in different aspects: Biota and Cretaceous environments of the La Buitrera Paleontological Area (Cerro Polic a, R o Negro, Argentina)”

PICT 2018-04598; Dinosaurs and associated fauna from “La Buitrera: the Patagonian Gobi” (early Late Cretaceous) Argentina (#8826-10) National Geographic Society.

## References

- Apesteuguía, S. 2005. A Late Campanian sphenodontid (Reptilia, Diapsida) from northern Patagonia. *Comptes Rendus Palevol* 4: 663–669.
- Apesteuguía, S. 2007. La evolución de los lepidosaurios. *Investigación y Ciencia* 367: 54–63.
- Apesteuguía, S. 2008. *Esfenodontes (Reptilia: Lepidosauria) del Cretácico Superior de Patagonia*. 545 pp. Ph.D. Thesis, Facultad de Ciencias Naturales y Museo, Universidad Nacional de La Plata, La Plata.
- Apesteuguía, S. and Jones, M.E.H. 2012. A Late Cretaceous “tuatara” (Lepidosauria: Sphenodontinae) from South America. *Cretaceous Research* 34: 154–160.
- Apesteuguía, S. and Novas, F.E. 2003. Large Cretaceous sphenodontian from Patagonia provides insight into lepidosaur evolution in Gondwana. *Nature* 425: 609–612.
- Apesteuguía, S. and Rougier, G.W. 2007. A late Campanian sphenodontid maxilla from northern Patagonia. *American Museum Novitates* 3581: 1–11.
- Apesteuguía, S., Gómez, R.O., and Rougier, G.W. 2012. A basal sphenodontian (Lepidosauria) from the Jurassic of Patagonia: new insights on the phylogeny and biogeography of Gondwanan rhynchocephalians. *Zoological Journal of the Linnean Society* 166: 342–360.
- Bonaparte, J.F. and Sues, H.D. 2006. A new species of *Clevosaurus* (Lepidosauria: Rhynchocephalia) from the Upper Triassic of Brazil. *Palaeontology* 49: 917–923.
- Buffrénil, V. and Castanet, J. 2000. Age estimation by skeletochronology in the Nile Monitors (*Varanus niloticus*), a highly exploited species. *Journal of Herpetology* 34: 414–424.
- Buffrénil, V. and Houssaye, A. 2021. Lepidosauria. In: V. De Buffrénil, A. De Ricqlès, L. Zylberberg, and K. Padian (eds.), *Vertebrate Skeletal Histology and Paleohistology*, 399–424. CRC Press, Boca Raton.
- Buffrénil, V. and Quilhac, A. 2021. Bone Remodeling. In: V. De Buffrénil, A. De Ricqlès, L. Zylberberg, and K. Padian (eds.), *Vertebrate Skeletal Histology and Paleohistology*, 229–246. CRC Press, Boca Raton.
- Caetano, M.H. 1990. Use and results of skeletochronology in some urodeles (*Triturus marmoratus*, Latreille 1800 and *Triturus boscai*, Lataste 1879). *Annales des sciences naturelles. Zoologie 13e Série* 11: 197–199.
- Castanet, J. and Baez, M. 1991. Adaptation and evolution in *Gallotia* lizards from the Canary Islands: age, growth, maturity and longevity. *Amphibia-Reptilia* 12: 81–102.
- Castanet, J., Curry Rogers, K., Cubo, J., and Boisard, J.-J. 2000. Periosteal bone growth rates in extant ratites (ostriche and emu). Implications. For assessing growth in dinosaurs. *Life Science* 323: 543–550.
- Castanet, J., Francillon-Vieillot H., Meunier, P.J., and Ricqlès, A. 1993. Bone and individual aging. In: B.K. Hall (ed.), *Bone*, 245–283. CRC Press, London.
- Castanet, J., Newman, D.G., and Saint Girons, H. 1988. Skeletochronological data on the growth, age, and population structure of the tuatara, *Sphenodon punctatus*, on Stephens and Lady Alice Islands, New Zealand. *Herpetologica* 44: 25–37.
- Chinsamy, A. and Hurum, J.H. 2006. Bone microstructure and growth patterns of early mammals. *Acta Palaeontologica Polonica* 51: 325–338.
- Chinsamy Turan, A. 2005. *The Microstructure of Dinosaur Bone: Deciphering Biology with Fine Scale Techniques*. 224 pp. Johns Hopkins University Press, Baltimore.
- Daugherty, C.H., Cree, A., Hay, J.M., and Thompson M.B. 1990. Neglected taxonomy and continuing extinctions of tuatara (*Sphenodon*). *Nature* 347: 177–179.
- Erickson, G.M. 2014. On dinosaur growth. *Annual Review of Earth and Planetary Sciences* 42: 675–697.
- Evans, S.E. and Jones, M.E.H. 2010. The origin, early history and diversification of lepidosauromorph reptiles. In: S. Bandyopadhyay (ed.), *New Aspects of Mesozoic Biodiversity*, 27–44. Springer-Verlag, Berlin.
- Francillon-Vieillot, H., de Buffrénil, V., Castanet, J., Géraudie, J., Meunier, F.J., Sire, J. Y., Zylberberg, L., and de Ricqlès, A. 1990. Microstructure and mineralization of vertebrate skeletal tissues. In: J.G. Carter (ed.), *Skeletal Biomineralization: Patterns, Processes and Evolutionary Trends 1*, 471–530. Van Nostrand Reinhold, New York.
- Gentil, A.R., Agnolin, F.L., García Marsà, J.A., Motta, M.J. and Novas, F.E. 2019. Bridging the gap: Sphenodont remains from the Turonian (Upper Cretaceous) of Patagonia. *Palaeobiological inferences. Cretaceous Research* 98: 72–83.
- Griffiths, I. 1961. Skeletal lamellae as an index of age in heterothermous tetrapods. *Annals and Magazine of Natural History, Series 13* 4: 449–465.
- Horner, J.R., de Ricqlès, A., and Padian, K. 1999. Variation in dinosaur skeletochronology indicators: implications for age assessment and physiology. *Paleobiology* 25: 295–304.
- Hsiou, A.S., De França, M.A.G., and Ferigolo, J. 2015. New data on the *Clevosaurus* (Sphenodontia: Clevosauridae) from the Upper Triassic of southern Brazil. *PLoS One* 10 (9): e0137523.
- Huttenlocker, A.K., Woodward, H.N., and Hall, B.K. 2013. The biology of bone. In: K. Padian, and E.T. Lamm (ed.), *Bone Histology of Fossil Tetrapods: Advancing Methods, Analysis and Interpretation*, 13–34. University of California Press, Berkeley.
- Hutton, J.M. 1986. Age determination of living Nile crocodiles from the cortical stratification of bone. *Copeia* 2: 332–341.
- Khonsue, W., Chaiananporn, T., and Pomchote, P. 2010. Skeletochronological assessment of age in the Himalayan crocodile newt, *Tylosotriton verrucosus* (Anderson, 1871) from Thailand. *Tropical Natural History* 10: 181–188.
- Klein, N. and Scheyer, T.M. 2017. Microanatomy and life history in *Palaeopleurosaurus* (Rhynchocephalia: Pleurosauridae) from the Early Jurassic of Germany. *The Science of Nature* 104: 1–8.
- Leanza, H.A., Apesteuguía, S., Novas, F.E. and de la Fuente, M.S. 2004. Cretaceous terrestrial beds from the Neuquén Basin (Argentina) and their tetrapod assemblages. *Cretaceous Research* 25: 61–87.
- LeBlanc, A.R., Apesteuguía, S., Larsson, H.C., and Caldwell, M.W. 2020. Unique tooth morphology and prismatic enamel in Late Cretaceous sphenodontians from Argentina. *Current Biology* 30: 1755–1761.
- Martinelli, A.G. and Forasiepi, A.M. 2004. Late Cretaceous vertebrates from Bajo de Santa Rosa (Allen Formation), Río Negro Province, Argentina, with the description of a new sauroid dinosaur (Titanosauridae). *Revista del Museo Argentino de Ciencias Naturales* 6: 257–305.
- Martínez, R.N., Apaldetti, C., Colombi, C.E., Praderio, A., Fernández, E., Malnis, P.S., Correa, G.A., Albelin, D., and Alcober, O. 2013. A new sphenodontian (Lepidosauria: Rhynchocephalia) from the Late Triassic of Argentina and the early origin of the herbivore opisthodontians. *Proceedings of the Royal Society B: Biological Sciences* 280: 20132057.
- Meier, P.S., Bickelmann, C., Scheyer, T.M., Koyabu, D., and Sánchez-Villagra, M.R. 2013. Evolution of bone compactness in extant and extinct moles (Talpidae): exploring humeral microstructure in small fossorial mammals. *BMC Evolutionary Biology* 13 (1): 1–10.
- Melchor, R., Perez, M., Villegas, P., Espinoza, N., Umazano, A., and Cardonatto, M.C. 2023. Early Cretaceous lepidosaurs (sphenodontian?) burrows. *Nature: Scientific Reports* 1: 310209.
- Montori, A. 1990. Skeletochronological results in the Pyrenean newt *Euproctus asper* (Dugés, 1852) from the pyrenean population. *Annales des sciences naturelles. Zoologie 13ème Série* 11: 209–211.
- Pereyra, M.E., Bona, P., Cerda, I.A., and Desántolo, B. 2019. Osteohistological correlates of muscular attachment in terrestrial and freshwater Testudines. *Journal of Anatomy* 234: 875–898.
- Ponce, D., Desojo, J.B., and Cerda, I.A. 2022. Palaeobiological inferences of the aetosaur *Aetosauroides scagliai* (Archosauria: Pseudosuchia) based on microstructural analyses of its appendicular bones. *Historical Biology* 35: 303–314.
- Rasband, W.S. 2003. *Image J*. National Institutes of Health, Bethesda, Maryland [available online, <http://rsb.info.nih.gov/ij/>].

- Reynoso, V.H. 1996. A Middle Jurassic Sphenodon-like sphenodontian (Diapsida: Lepidosauria) from Huizachal Canyon, Tamaulipas, Mexico. *Journal of Vertebrate Paleontology* 16: 210–221.
- Reynoso, V.H. 2003. Growth patterns and ontogenetic variation of the teeth and jaws of the Middle Jurassic sphenodontian *Cynosphenodon huizachalensis* (Reptilia: Rhynchocephalia). *Canadian Journal of Earth Sciences* 40: 609–619.
- Ricqlès, A. and Gayon, J. 2015. Function. In: T. Heams, P. Huneman, G. Lecointre, and M. Silberstein (eds.), *Handbook of Evolutionary Thinking in the Sciences*, 95–112. Springer, Dordrecht.
- Ricqlès, A., Meunier, F.J., Castanet, J., Francillon-Vieillot, H., and Hall, B.K. 1991. Bone matrix and bone specific products. In: B.K. Hall (ed.), *Bone* 3: 1–78. CRC Press, Boca Raton.
- Schucht, P.J., Klein, N., and Lambertz, M. 2021. What's my age again? On the ambiguity of histology-based skeletochronology. *Proceedings Royal Society B* 288: 20211166.
- Simón, M.E. and Kellner, A.W.A. 2003. New sphenodontid (Lepidosauria, Rhynchocephalia, Eilenodontinae) from the Candeleros Formation, Cenomanian of Patagonia, Argentina. *Boletim Museu Nacional, nova série* 68: 1–12.
- Waskow, K. and Sander, M. 2014. Growth record and histological variation in the dorsal ribs of *Camarasaurus* sp. (Sauropoda). *Journal of Vertebrate Paleontology* 34: 852–869.
- Whiteside, D.I. 1986. The head skeleton of the Rhaetian sphenodontid *Diphydontosaurus avonis* gen. et sp. nov. *Philosophical Transactions of the Royal Society of London B: Biological Sciences* 312: 379–430.